HEFAT2014
10th International Conference on Heat Transfer, Fluid Mechanics and Thermodynamics
14 - 26 July 2014
Orlando, Florida

TWO HERMITE ANALOGS OF THE LOWEST ORDER RAVIART-THOMAS MIXED ELEMENT FOR THE CONVECTION-DIFFUSION EQUATIONS

V. Ruas* and P. Trales†
*CNPq scholar, Graduate School of Metrology for Quality and Innovation,
Pontifícia Universidade Católica do Rio de Janeiro,
Rio de Janeiro,
Brazil,
&
Sorbonne Universités, UPMC, UMR 7190, Institut Jean Le Rond d'Alembert, CNRS,
Paris,
France,
E-mail: vitoriano.ruas@pq.cnpq.br
†Instituto de Matemática e Estatística, Universidade Federal Fluminense,
Niterói, Rio de Janeiro state,
Brazil,
E-mail: paulotrales@im.uff.br

ABSTRACT

[1]This work addresses two techniques to solve convection-diffusion problems based on Hermite interpolation. More specifically it deals with an adaptation to the case of these equations of a Hermite finite element method providing flux continuity across inter-element boundaries, shown to be an efficient tool for simulating purely diffusive phenomena [7]. In the latter case the method is the Hermite analog of the celebrated lowest order Raviart-Thomas mixed finite element method known as RT_0 [5]. The new methods in turn can be viewed as non trivial improved versions of the RT_0 extensions to convection-diffusion problems, in divergence form or not, proposed by Douglas and Roberts [3] more than three decades ago. In contrast to the mixed methods, second order convergence results in the mean square sense are proven to hold for both Hermite finite element approaches, and comparative numerical results illustrate the good performance of the new methods.

[1]Work supported by CNPq, Brazil, through grant 307996/2008-5.

Keywords: Convection, diffusion, finite elements, Hermite, Raviart-Thomas

INTRODUCTION

Many numerical techniques are available nowadays to simulate physical phenomena involving both convection and diffusion processes, such as heat transfer and fluid flow. Generally speaking, any efficient numerical approach in this framework must be able to solve in a reliable manner, the linear scalar convection-diffusion equation, since they lie on the basis of the mathematical modeling of countless technological or scientific problems. This fact keeps encouraging specialists in the search for efficient methodology to solve these equations. This is particularly true of convection dominated processes, in which the correct capture of sharp boundary layers often reveal demerits of widespread computational techniques, even when the problem to solve is linear. As far as numerical methods allowing for the representation of diffusive fluxes

across the boundaries of discretization cells are concerned, both mixed finite elements and finite volumes have been playing a prominent role since long. This is because very often in current applications the fluxes are more important than the primal unknown itself. Among them one could quote flow in porous media as an outstanding application. However Hermite interpolation can also be a tool well adapted to the enforcement of such a continuity property, as shown in [7] for pure diffusion equations in highly heterogeneous media. In that work two finite element methods of the Hermite type based on a quadratic interpolation were studied. Both have, either identical or better convergence properties than some of the classical mixed methods, such as the RT_0 method, i.e. the lowest order Raviart-Thomas' [5], according to the norm under consideration, though at comparable implementation cost. Actually it turned out from numerical experiments that these Hermite methods are able to produce very accurate solutions, in particular as far as the error of the primal unknown measured in L^p-norms are concerned.

In [8] the authors extended to the case of the convection-diffusion equation, the Hermite finite element first studied in [6], that can be regarded as a variant of the lowest order Raviart-Thomas mixed element for the pure diffusion equation. The purpose of this work is two-fold: first of all the authors complete the study of such an extension, and then they consider a different version of it. Actually the two versions of the extension of RT_0 to the convection-diffusion equations studied here can be viewed as Hermite analogs of the two mixed extensions of the RT_0 method to linear second order elliptic equations proposed by Douglas and Roberts in [3], restricted to the case of the linear convection-diffusion equation. The method proposed in [8] corresponds to the mixed method studied in [3] for the equations in non divergence form, and the one introduced here can be viewed as an analogue of the mixed method considered in [3] for the equations in divergence form. Similarly to [6], a priori error estimates in the L^2-norm are in terms of the square of the mesh size for both Hermite methods, in contrast to the first order ones that hold for the RT_0 or the Douglas and Roberts mixed methods. In this work the authors extend to the case of the convection-diffusion equations, the Hermite finite element that can be regarded as a variant of the lowest order Raviart-Thomas mixed element [6]. Here again a priori error estimates in the L^2-norm are in terms of the square of the mesh size, in contrast to the first order ones that hold for the extension of the RT_0 method to C-D equations proposed in [3].

For the purpose of this work one may work with the convection-diffusion equation in dimensionless form without specification of the application in view. However for the sake of clarity one might consider the case where the unknown function u is a temperature. In this case the notations employed here correspond to quantities playing a prominent role in a heat transfer process by convection and conduction, i.e. diffusion :

NOMENCLATURE

u [K]: Temperature
x_1 [m]: Cartesian axis direction
x_2 [m]: Cartesian axis direction
x_3 [m] : Cartesian axis direction
L [m] : Characteristic length of the heat transfer domain.
$\mathcal{K}$ [W/mK]: Tensor of (anisotropic) thermal conductivity
$\mathbf{w}$ [m/s] : Convective velocity
f [W/m^3] : Volumetric density of heat generation
Pé : Péclet number.

In all the sequel the authors study as a model the following equation assumed to have a unique solution u in a (heat flow) bounded domain Ω of $\Re^N$, $N = 2, 3$, with boundary Γ:
Let the source function f be given in $L^2(\Omega)$ together with tensor $\mathcal{K}$ assumed to be constant, symmetric and positive definite and the velocity $\mathbf{w}$ in $\mathbf{C}^0(\bar{\Omega})$. Denoting by ∇ and $\nabla\cdot$ the gradient and the divergence operator, respectively, one wishes to:

$$\text{Find } u \in H_0^1(\Omega) \text{ such that } -\nabla\cdot\mathcal{K}\nabla u + \mathbf{w}\cdot\nabla u = f \text{ in } \Omega. \tag{1}$$

Henceforth let be assumed that Ω is a polygon if $N = 2$ or a polyhedron if $N = 3$, and that a finite element partition $\mathcal{T}_h$ of Ω is given, consisting of triangles or tetrahedra according to the value of N, and belonging to a quasi-uniform family of partitions (cf. [4]). h denotes the maximum diameter of the elements of $\mathcal{T}_h$. Referring to [1], in the sequel the following notations are employed: S being a bounded open set of $\Re^N$, the standard norm of Sobolev spaces $H^m(S)$ (resp. $W^{m,p}(S)$ for $p \geq 1$, $p \neq 2$), for any non negative integer m is denoted by $\|\cdot\|_{m,S}$ (resp. $\|\cdot\|_{m,p,S}$), including $L^2(S) = H^0(S)$. The standard semi-norm of $H^m(\Omega)$ (resp. $W^{m,p}(S)$ for $p \geq 1$, $p \neq 2$) is denoted by $|\cdot|_{m,S}$ (resp. $|\cdot|_{m,p,S}$).

THE METHOD FOR C-D EQUATIONS IN NON DIVERGENCE FORM

In this Section the authors recall their method introduced in [8], applying to the convection-diffusion equations in non divergence form.

To begin with let U_h and V_h be two finite element spaces associated with $\mathcal{T}_h$ defined as follows: Let $\mathbf{w}_h$ be the constant field in each element of $T \in \mathcal{T}_h$ whose value in T is $\mathbf{w}(G_T)$, where G_T is the centroid of T, and $\mathbf{w}_h^1$ be the standard continuous piecewise linear interpolate of $\mathbf{w}$ at the vertices of $\mathcal{T}_h$. The operators $\Pi_T : L^2(T) \longrightarrow L^2(T)$ given by $\Pi_T[v] := \int_T v dx/meas(T)$ for $T \in \mathcal{T}_h$, and $\Pi_h : L^2(\Omega) \longrightarrow L^2(\Omega)$ by $\Pi_h[v]_{|T} = \Pi_T[v_{|T}]$ $\forall T \in \mathcal{T}_h$ are further introduced.
Every function $v \in V_h$ or $u \in U_h$ is such that in each element $T \in \mathcal{T}_h$ it is expressed by $\mathbf{x}^t \mathcal{K}^{-1}[a\mathbf{x}/2+\mathbf{b}]+d$, where $\mathbf{x}$ represents the space variable, $\mathbf{b}$ is a constant vector of $\Re^N$ and a and d are two real coefficients. Now F being an edge if $N = 2$ or a face if $N = 3$ belonging to the boundary ∂T of an element $T \in \mathcal{T}_h$, and $\mathbf{n}_F$ being the unit normal vector on F oriented in a unique manner for the whole mesh, in this work every function in $v \in V_h$ (resp. $u \in U_h$) is such that its restriction to any $T \in \mathcal{T}_h$ is defined by means of $N + 1$ degrees of freedom, namely, the N mean values of the flux $(\mathcal{K}\nabla v+\mathbf{w}_h\Pi_T[v])\cdot\mathbf{n}_F$ (resp. $(\mathcal{K}\nabla u)\cdot\mathbf{n}_F$) over $F \subset \partial T$, and $\Pi_T[v]$ (resp. $\Pi_T[u]$). All the degrees of freedom of the first type coincide on both sides of every interface F common to two elements of $\mathcal{T}_h$. The canonical basis functions for these spaces corresponding to the above degrees of freedom can be determined as follows. First notice that $\forall v \in V_h$ or $u \in U_h$, the fluxes are constant over every edge or face F of any element T of the mesh. Indeed from the particular form of $v_{|T}$ or $u_{|T}$, both ∇v and ∇u are of the form $\mathcal{K}^{-1}[a\mathbf{x} + \mathbf{b}]$. Then the flux is of the form $a\mathbf{x}+\mathbf{c}$, and from a well-known property of the lowest order Raviart-Thomas mixed element, whose flux variable is locally defined by functions of the same form, the result follows. Incidentally this allows for the determination of a and $\mathbf{c}$ for each basis function corresponding to a given flux, in the same way as for the flux basis functions corresponding to the lowest order Raviart-Thomas element. This yields the value of $\mathbf{b}$, d being adjusted in such a way that $\Pi_T[v] = \Pi_T[u] = 0$ and the flux basis functions are thus uniquely defined. As for the basis function corresponding to the second type of degree of freedom, $a = 0$ for both v and u, while $\mathbf{b} = -\mathbf{w}_h$ and $d = 1 + [\mathbf{w} \cdot \mathbf{x}](G_T)$ for v, and $\mathbf{b} = \mathbf{0}$ and $d = 1$ for u.

Next the discrete variational problem (2) is set below, in the aim of approximating (1), whose bilinear form a_h and linear form L are given by (3), the notation $(p, q)_S$ representing $\int_S pq\, dS\ \forall S \subset \Omega,\ p, q \in L^2(S)$.

$$\begin{aligned} &\text{Find } u_h \in U_h \text{ such that } a_h(u_h, v) = L_h(v)\ \forall v \in V_h \\ &\text{where } \forall u \in U_h \text{ and } \forall v \in V_h, \end{aligned} \tag{2}$$

$$\begin{cases} a_h(u,v) := & \sum_{T\in\mathcal{T}_h} \big[(\nabla\cdot\mathcal{K}\nabla u - \mathbf{w}_h^1\cdot\nabla u, \Pi_T[v])_T + \\ & (\nabla u, \mathcal{K}\nabla v + \mathbf{w}_h\Pi_T[v])_T + (u, \nabla\cdot\mathcal{K}\nabla v)_T\big]; \\ L_h(v) := & -(f, \Pi_h[v])_\Omega. \end{cases} \tag{3}$$

If V is the space given by $V := \{v | v \in H^1(\Omega); \nabla\cdot\mathcal{K}\nabla v \in L^2(\Omega)\}$, form a_h can be extended to $(U_h + V) \times (V_h + V)$. Then one may further introduce the functional $\| \cdot \|_h$: $U_h + V_h + V \longrightarrow \Re$ given by: $\| v \|_h^2 := (\Pi_h[v], \Pi_h[v])_\Omega + \sum_{T\in\mathcal{T}_h} \{(\nabla v, \nabla v)_T + (\nabla\cdot\mathcal{K}\nabla v, \nabla\cdot\mathcal{K}\nabla v)_T\}$. The expression $\| \cdot \|_h$ obviously defines a norm over V, U_h and V_h.
In this manner, it is easy to establish the continuity of a_h over $(U_h+V)\times(V_h+V)$ with a mesh independent constant M. In [8] the authors proved the validity of the following inf-sup condition for a_h over $U_h \times V_h$ [5], which implies that (2) has a unique solution.

Proposition 4.1 *[8] If h is sufficiently small and $\mathbf{w} \in W^{1,\infty}(\Omega)$, there exists a constant $\alpha > 0$ independent of h such that*

$$\forall u \in U_h \setminus \{0\} \quad \sup_{v\in V_h\setminus\{0\}} \frac{a_h(u,v)}{\| v \|_h} \geq \alpha \| u \|_h . \tag{4}$$

■

In [8] the following a priori error estimate was also proven to hold :

Theorem 4.2 *Assume that $\mathbf{w} \in W^{1,\infty}(\Omega)$ and h is sufficiently small. Then if $u \in H^2(\Omega)$ and $f \in H^1(\Omega)$ there exists a mesh independent constant C' such that,*

$$\| u - u \|_h \leq C' h\, [|u|_{2,\Omega} + |f|_{1,\Omega}]. \tag{5}$$

■

The main property of the method described in this Section is given in the following Theorem.

Theorem 4.3 *If Ω is convex, $\mathbf{w} \in W^{1,\infty}(\Omega)$ and h is sufficiently small, there exists a constant $C^{''}$ independent of h such that,*

$$\| u - u_h \|_{0,\Omega} \leq C^{''} h^2 \, [|u|_{2,\Omega} + |f|_{1,\Omega}]. \tag{6}$$

■

The proof of Theorem 4.3 is based on the same arguments as those employed to prove Theorem 2.3 of [6]. However notice that some additional technicalities come into play in the case of the convection-diffusion equation. For this reason the complete proof of this result, together with analogous ones related to the other method presented in this work, will be the object of a forthcoming paper.

THE METHOD FOR C-D EQUATIONS IN DIVERGENCE FORM

Before introducing this method it is wise to rewrite equation (1) in divergence form, namely,

$$\left\{ \begin{array}{l} \text{Find } u \in H_0^1(\Omega) \text{ and } \mathbf{p} \in \mathbf{H}(div;\Omega) \text{ such that} \\ \nabla \cdot \mathbf{p} - \nabla \cdot \mathbf{w}\, u = f \text{ in } \Omega, \\ \mathbf{p} = -\mathcal{K}\nabla u + \mathbf{w}u. \end{array} \right. \tag{7}$$

where $\mathbf{H}(div;\Omega) := \{\mathbf{q} \mid \mathbf{q} \in [L^2(\Omega)]^N,\ \nabla \cdot \mathbf{q}\ \in L^2(\Omega)\}$.

A natural weak (variational) formulation equivalent to system (7) is given in [3], that is,

$$\left\{ \begin{array}{l} \text{Find } u \in L^2(\Omega) \text{ and } \mathbf{p} \in \mathbf{H}(div;\Omega) \text{ such that} \\ (\nabla \cdot \mathbf{p}, v)_\Omega - (\nabla \cdot \mathbf{w}\, u, v)_\Omega = (f, v)_\Omega \ \forall v \in L^2(\Omega), \\ (\mathcal{K}^{-1}\mathbf{p}, \mathbf{q})_\Omega - (u, \nabla \cdot \mathbf{q})_\Omega - (\mathcal{K}^{-1}\mathbf{w}\, u, \mathbf{q})_\Omega = 0 \\ \forall \mathbf{q} \in \mathbf{H}(div;\Omega). \end{array} \right. \tag{8}$$

The extension of RT_0 to the C-D equation considered in [3] consists of using the Raviart-Thomas interpolation of the lowest order to represent $\mathbf{p}$ and $\mathbf{q}$ - i.e. to approximate $\mathbf{H}(div;\Omega)$ -, and the space of constant functions in each element of the partition $\mathcal{T}_h$ to represent u and v. In contrast, here the authors shall mimic (8) by resorting to the space U_h, after adding up both relations in (8). More specifically they take in each element $T \in \mathcal{T}_h$, $\mathbf{q}_{|T} = \mathcal{K}\nabla v_{|T}$ for $v \in U_h$, and define the space W_h of functions of the form $\mathbf{x}^{\mathrm{t}}\mathcal{K}^{-1}[a\mathbf{x}/2 + \mathbf{b}] + d$ in each $T \in \mathcal{T}_h$, such that the normal component of $-\mathcal{K}\nabla u + \tilde{\mathbf{w}}\Pi_h[u]$ is continuous across all the inner edges of the partition. In order to allow the feasibility of such a construction the field $\tilde{\mathbf{w}}$ must be of the form $c\mathbf{x} + \mathbf{d}$ in each $T \in \mathcal{T}_h$ for suitable real numbers $c, d_1, \ldots, d_N$, $\mathbf{d} = [d_1, \ldots, d_N]$. The choice of $\tilde{\mathbf{w}}$ compatible with the continuity of the normal component of the flux variable $\mathbf{p} = -\mathcal{K}\nabla u + \mathbf{w}u$ across the edges is certainly the interpolate of $\mathbf{w}$ in the Raviart-Thomas (RT_0) space, and this completes the definition of W_h.
Now replace in (8) :

- u with $\Pi_h[u_h]$, if the gradient operator is not directly applied to it ;
- ∇u with ∇u_h;
- $\mathbf{w}$ with $\tilde{\mathbf{w}}$ if the divergence operator is not directly applied to it;
- $\mathbf{p}$ with $-\mathcal{K}\nabla u_h + \tilde{\mathbf{w}}\Pi_h[u_h]$ (taking $u_h \in W_h$);
- $\mathbf{q}$ with $-\mathcal{K}\nabla v$ (taking $v \in U_h$);
- f with $\Pi_T[f]$ in every $T \in \mathcal{T}_h$.

This leads to the following equation:

$$\begin{array}{l} \sum_{T\in\mathcal{T}_h} [(\nabla \cdot \{\mathcal{K}\nabla u_h - \tilde{\mathbf{w}}\Pi_T[u_h]\}, v)_T + (\nabla \cdot \mathbf{w}\Pi_T[u_h], v)_T + \\ (\mathcal{K}\nabla u_h - \tilde{\mathbf{w}}\Pi_T[u_h], \nabla v)_T + (\Pi_T[u_h], \nabla \cdot \mathcal{K}\nabla v)_T \\ +(\tilde{\mathbf{w}}\Pi_T[u_h], \nabla v)_T] = -(\Pi_h[f], v)_\Omega \ \forall v \in U_h \end{array} \tag{9}$$

After straightforward simplifications, and taking into account that $(\Pi_h[f], v)_\Omega = (f, \Pi_h[v])_\Omega$, the following Hermite finite element counterpart of (1) can be defined:

Find $u_h \in W_h$ such that $\tilde{a}_h(u_h, v) = L_h(v)\ \forall v \in U_h$ where $\forall u \in W_h$ and $\forall v \in U_h$, (10)

$$\left\{ \begin{array}{l} \tilde{a}_h(u, v) := \sum_{T\in\mathcal{T}_h} [(\nabla \cdot \{\mathcal{K}\nabla u - \tilde{\mathbf{w}}\ \Pi_T[u_h]\}, v)_T + \\ (\nabla \cdot \mathbf{w}\Pi_T[u_h], v)_T + (\nabla u, \mathcal{K}\nabla v)_T + (u, \nabla \cdot \mathcal{K}\nabla v)_T] \end{array} \right. \tag{11}$$

The fact that problem (10) has a unique solution can be established quite similarly to problem (2). The convergence results that hold for this method can be proved very much like in the case of the method of the previous section. The main difference is that it is necessary to reguire

a little more regularity of $\nabla \cdot \mathbf{w}$, namely, that this function lies in $W^{1,\infty}(\Omega)$. Apart from this assumption, the results are qualitatively equivalent, in the sense that a priori error estimates completely analogous to those of Theorems 4.2 and 4.3 apply to problem (10) as well. The corresponding analysis will be the object of a forthcoming paper. As far as this work is concerned, resulting properties among others the authors have not formally established, are illustrated by means of a series of numerical examples.

COMPARATIVE NUMERICAL EXPERIMENTS

Several numerical results were obtained with the methods described in the two previous sections. Some of them are supplied below for academic test problems, which particularly highlight the behavior of both Hermite methods. In the tests manufactured solutions u are given, which together with $\mathcal{K}$ and $\mathbf{w}$ produce right hand side data f. For comparative purposes the test problems were also solved with the Douglas & Roberts RT_0 element [3] in its two versions for equation (1) - that is, for its formulation in divergence form or not [3], referred to as RT_{0b} and RT_{0a} respectively. Their Hermite analogs in turn are referred to as RT_{0d} and RT_{0c} respectively. In all the test problems $\mathcal{K}$ is chosen to be $\mathcal{I}$ and domains with characteristic length $L = 1$ are considered. In this case the Péclet number can be defined by Pé$= \max|\mathbf{w}(\mathbf{x})|$ for $\mathbf{x} \in \Omega$.

In the first battery of tests Ω is the disk with unit radius and center at the origin of the cartesian coordinates x_1 and x_2. For symmetry reasons in the computations only the quarter of disk defined by the positive values of both coordinates is taken into account. The purpose of these tests is to observe the behavior of all four solution methods in the presence of a curved boundary approximated by a polygon, that is, the union of the mesh triangles. For this reason $\mathbf{w}$ is chosen to be Pé$(-x_2; x_1)$, which incidentally annihilates the effects of the term involving the divergence of $\mathbf{w}$. Furthermore $u(x_1, x_2) = (1 - x_1^2 - x_2^2)/4$ is selected, for this function can be represented exactly by the Hermite elements RT_{0c} and RT_{0d}, though only in the polygons approximating Ω. The computational meshes consist of $2l^2$ triangles constructed as described in [9], where l is a strictly positive integer. Notice that by this process the generated meshes are pseudo-uniform, in the sense that the elements are very similar to each other in both shape and size. Here is chosen to be of the form $l = 2^m$ for $m = 3, 4, 5, 6$, which yields values of h greater than or equal to l^{-1} and less than $\sqrt{\pi^2 + 16}/4\ l^{-1}$ for all l [9]. These simulations are referred to hereafter as Test-problem 1.

Tables 1, **2** and **3** display the errors measured in the L^2-norm of the approximations of u, ∇u and the divergence of the flux referred to as $DF(u)$ hereafter, obtained with the four methods RT_{0a}, RT_{0c}, RT_{0b} and RT_{0d} as h decreases, for Pé$= 1$. Notice that $DF(u)$ equals Δu for the four methods, except for RT_{0b}, in which case it is given by $\nabla \cdot [\mathcal{K}\nabla u - \mathbf{w}u]$. In **Tables 4**, **5** and **6** the same kind of results are supplied for Pé$= 10^6$.

For a small Péclet number the numerical solutions are certainly likely to behave in a more coherent way with respect to expected theoretical predictions. For this reason the first comments are related to the results for Pé$= 1$. As one infers from **Table 1** and **Table 2**, the

l	RT_{0a}	RT_{0b}	RT_{0c}	RT_{0d}
8	0.92106378E-02	0.12088608E-01	0.14273321E-03	0.72878159E-08
16	0.46131717E-02	0.91517998E-02	0.36641214E-04	0.73099739E-08
32	0.23075591E-02	0.82633266E-02	0.92227890E-05	0.73155245E-08
64	0.11539009E-02	0.80263174E-02	0.23096840E-05	0.73169126E-08

Table 1: L^2 errors of u in Test 1 for Pé=1.

l	RT_{0a}	RT_{0b}	RT_{0c}	RT_{0d}
8	0.93229273E-08	0.49035715E-01	0.45950033E-02	0.93229273E-08
16	0.93341685E-08	0.48942597E-01	0.23211704E-02	0.93341684E-08
32	0.93369804E-08	0.48911400E-01	0.11636060E-02	0.93369804E-08
64	0.93376836E-08	0.48902954E-01	0.58218263E-03	0.93376836E-08

Table 2: L^2 errors of ∇u in Test 1 for Pé=1.

l	RT_{0a}	RT_{0b}	RT_{0c}	RT_{0d}
8	0.26390408E-07	0.26390408E-07	0.12129518E-01	0.26390408E-07
16	0.26406317E-07	0.26406317E-07	0.60914089E-02	0.26406317E-07
32	0.26410294E-07	0.26410294E-07	0.30490236E-02	0.26410294E-07
64	0.26411289E-07	0.26411289E-07	0.15249263E-02	0.26411289E-07

Table 3: L^2 errors of $DF(u)$ in Test 1 for Pé=1.

l	RT_{0a}	RT_{0b}	RT_{0c}	RT_{0d}
8	0.92106342E-02	0.80277062E+04	0.28468606E-07	0.85776730E-07
16	0.46131717E-02	0.41271521E+04	0.17701899E-07	0.24675365E-07
32	0.23075590E-02	0.20787739E+04	0.90843429E-08	0.12246846E-08
64	0.11539009E-02	0.10464045E+04	0.86802672E-08	0.51323208E-08

Table 4: L^2 errors of u in Test 1 for Pé=1.E+06

l	RT_{0a}	RT_{0b}	RT_{0c}	RT_{0d}
8	0.27348255E-06	0.12493936E+10	0.13313106E-06	0.22441098E-06
16	0.15627926E-07	0.47454176E+08	0.35134232E-07	0.69222706E-07
32	0.15255380E-07	0.80931090E+08	0.13704492E-07	0.10388122E-07
64	0.97826386E-08	0.20381309E+08	0.12701600E-07	0.39247399E-08

Table 5: L^2 errors of ∇u in Test 1 for Pé=1.E+06

l	RT_{0a}	RT_{0b}	RT_{0c}	RT_{0d}
8	0.16994514E-05	0.49306646E-06	0.42581852E-05	0.22408193E-05
16	0.31802766E-06	0.17720979E+01	0.32516391E-06	0.51235847E-06
32	0.83513808E-07	0.15533869E-06	0.71639581E-07	0.12256936E-06
64	0.37797137E-07	0.97959156E-07	0.41604712E-07	0.27102455E-07

Table 6: L^2 errors of $DF(u)$ in Test 1 for Pé=1.E+06

numerical solution is practically exact for the Hermite method RT_{0d}, while second order convergence to u and first order convergence to ∇u are observed for Hermite method RT_{0c}. One may conclude that the latter method is sensitive to the approximation of the curved boundary by polygonal lines, because otherwise the numerical solution would be exact up to round-off errors. On the other hand, **Tables 1** and **2** also show that the Raviart-Thomas mixed method in the Douglas & Roberts version RT_{0a} produces linear convergence to u and practically exact values of ∇u, while no clear convergence rates to these quantities can be observed for the version RT_{0b}. This seems to indicate that the curved boundary locks the convergence properties of the latter method, since in [3] it was proved to converge linearly in the case of polygonal domains. As for convergence to $DF(u)$, **Table 3** gives rise to somewhat surprising conclusions. Indeed, except for RT_{0c} all the methods yield practically exact values of this quantity independently of the mesh in use. Actually the linear convergence to Δu of the laplacian of RT_{0c} solutions, indicates here again how this method is affected by the boundary approximation.
The results obtained for Pé= 10^6 are quite different from those displayed in **Tables 1** through **3**. This is even more remarkable as far as the mixed methods RT_{0a} and RT_{0b} are concerned, for the latter method now generates completely meaningless results. Method RT_{0a} in turn is still first order convergent to u, but is now practically exact in terms of the computed values of ∇u and Δu. On the other hand both Hermite methods RT_{0c} and RT_{0d} are practically exact for all the three quantities being plotted. The authors have no explanation for such favorable behaviors, since they were not reproduced in other simulations, as seen from the test problems reported below.

In the second battery of tests Ω is the unit square $(0,1)\times(0,1)$ and $u(x_1,x_2)=(x_1-x_1^2)(x_2-x_2^2)/4$. Uniform meshes were employed with $2l^2$ triangles constructed by first subdividing Ω into l^2 equal squares and then subdividing each one of these squares into two triangles by means of the diagonal parallel to the line $x_1=x_2$. The corresponding value of h is $\sqrt{2}l^{-1}$. In the figures captions $\mathbf{w}$ is specified, together with the corresponding Péclet numbers. The first thing to be noted is that in each test case the results obtained with both Hermite methods are practically the same. Referring to the two previous sections the reader can notice that the main difference between both methods relies on the way of approximating $\mathbf{w}$ (by using either $\mathbf{w}_h$ and $\mathbf{w}_h^1$ or $\tilde{\mathbf{w}}$). This suggests that these different types of approximation play a negligible role in practice, in the case of a polygonal domain. Owing to this observation in the remainder of this Section both methods RT_{0c} and RT_{0d} will be referred to as HRT_0.
In Test-problem 2 the convergence properties of the methods under study are checked numerically, and in this aim m varies from 3 up to 6. Here $\mathbf{w}$ =Pé$\sqrt{2}(x_1;x_2)/2$ for increasing Péclet numbers, namely, Pé= $\sqrt{2}10^n/2$, for $n=0,2,4$. Next errors measured in the L^2-norm are shown for methods RT_{0a}, RT_{0b} and HRT_0, as h decreases. They are assigned to a figure with label **a** if they correspond to u, to a figure with label **b** if they refer to ∇u, and to a figure with label **c** if they are associated with $DF(u)$. **Figures 1**, **Figures 2** and **Figures 3** correspond to Pé= $0.5\sqrt{2}$, Pé= $50\sqrt{2}$ and Pé= $5,000\sqrt{2}$. The lines with slope 1. and 2. corresponding to h and h^2 are also drawn in the figures, so that convergence rates

can be better recognized.

Figure 1a

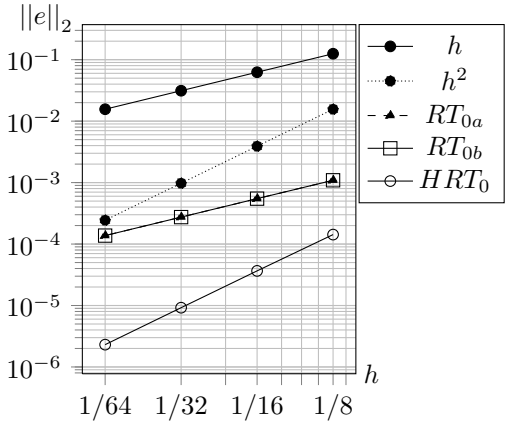

Figure 1: L^2 errors of u in Test 2 for Pé= $.5\sqrt{2}$.

Figure 1b

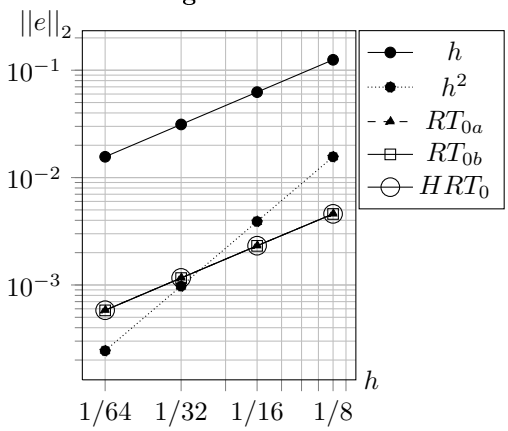

Figure 2: L^2 errors of ∇u in Test 2 for Pé= $.5\sqrt{2}$.

The displayed results can be summarized as follows: For lower Péclet numbers the methods behave exactly as predicted by the theoretical results given in the previous sections. More particularly **Figure 1a** and **Figure 2a** confirm that method HRT_0 is second order convergent in L^2 while methods RT_{0a} and RT_{0b} converge linearly. Moreover the solution gradient and laplacian converge linearly for all the three methods as predicted, according

Figure 1c

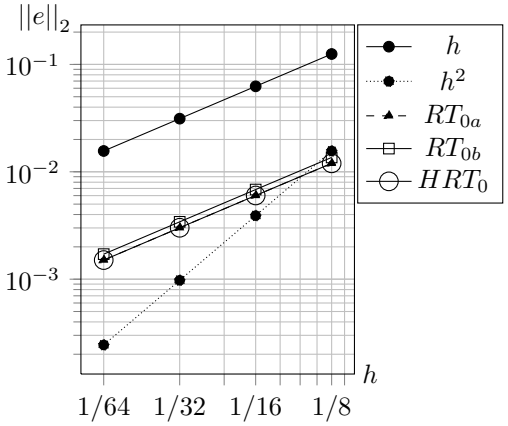

Figure 3: L^2 errors of $DF(u)$ in Test 2 for Pé=$.5\sqrt{2}$.

Figure 2a

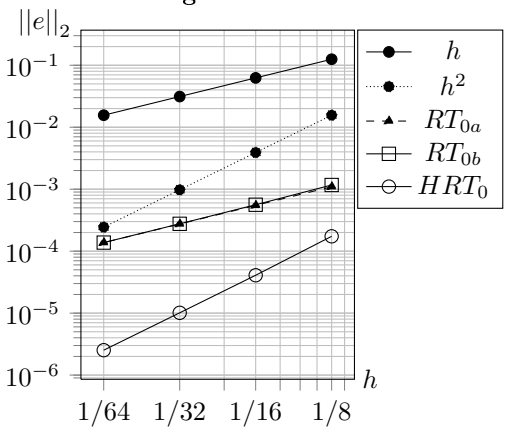

Figure 4: L^2 errors of u in Test 2 for Pé= $50.\sqrt{2}$.

to **Figures 1b**, **Figures 1c**, **Figures 2b**, **Figures 2c**. As far as accuracy is concerned, one observes that whenever the order of convergence is the same methods HRT_0 and RT_{0a} are practically equivalent - i.e. in gradient and laplacian computations -, and more accurate than RT_{0b}. As for results obtained for Pé= $5,000\sqrt{2}$ a completely different behavior is observed as shown in **Figure 3a**, **Figure 3b** and **Figure 3c**: methods RT_{0a} and HRT_0 diverge all the way, while method RT_{0b} converges for u, ∇u and $DF(u)$, though with unclear rates. Notice that the errors of the flux divergence are rather large for RT_{0b}, but this is normal since this variable is directly influenced

Figure 2b

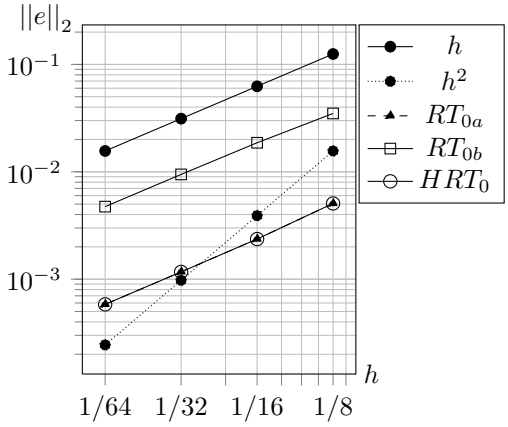

Figure 5: L^2 errors of ∇u in Test 2 for Pé$= 50.\sqrt{2}$.

Figure 2c

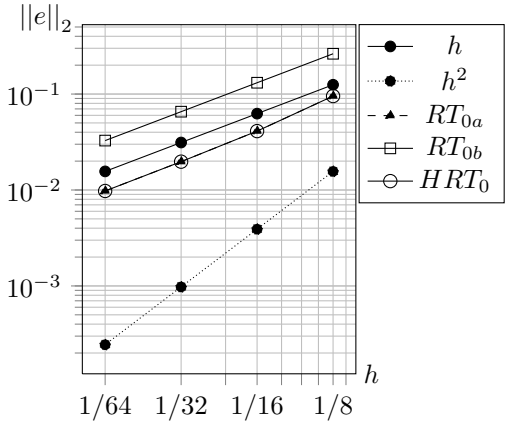

Figure 6: L^2 errors of $DF(u)$ in Test 2 for Pé$= 50.\sqrt{2}$.

Figure 3a

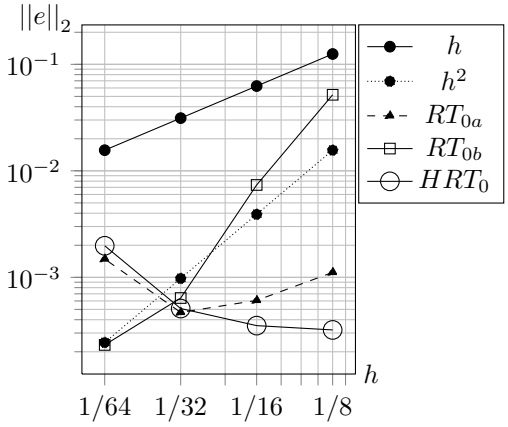

Figure 7: L^2 errors of u in Test 2 for Pé$= 5000.\sqrt{2}$.

Figure 3b

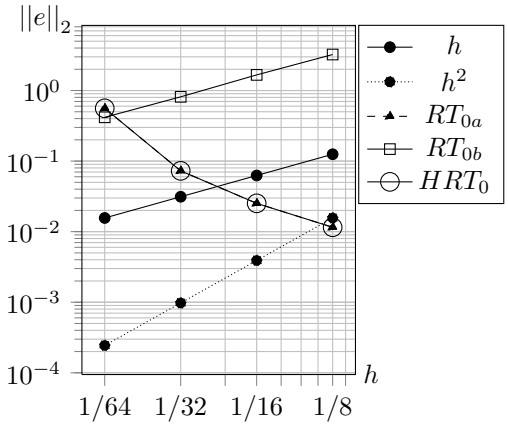

Figure 8: L^2 errors of ∇u in Test 2 for Pé$= 5000.\sqrt{2}$.

by the Péclet number.

The purpose of Test-problem 3 is to check the behavior of each one of the methods RT_{0a}, RT_{0b} and HT_0 as the Péclet number varies, keeping the mesh fixed. More precisely only the finest mesh among the above ones is considered, that is $l = 64$, while now $\mathbf{w} =$Pé$(x_1^2, x_2^2)/\sqrt{2}$. In **Figure 4**, **Figure 5** and **Figure 6** the L^2-errors of u, ∇u and $DF(u)$, respectively, are displayed, for Péclet numbers equal to $\sqrt{2}10^n$ where n ranges from 0 up to 4.

The conclusions to be drawn from these results can be summarized as follows. First of all one can say that for Péclet numbers up to the magnitude of about 10^3 method HRT_0 is qualitatively superior to both RT_{0a} and RT_{0b} as far as the errors of u are concerned, as expected. On the other hand methods HRT_0 and RT_{0a} are rather equivalent in terms of the approximations of ∇u and $DF(u)$, whereas RT_{0b} is fairly less accurate in both respects. The second observation to be reported is that the results obtained with HRT_0 and RT_{0a} downgrade for Pé greater than 10^4. This also happens to RT_{0b} but to a much lesser extent. This fact could advocate in favor of the latter method for high Péclet number simulations.

Figure 3c

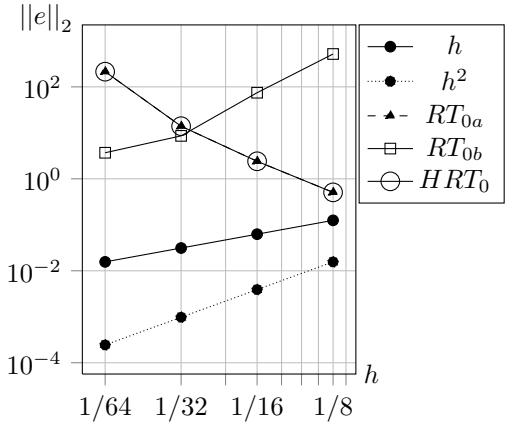

Figure 9: L^2 errors of $DF(u)$ in Test 2 for Pé$= 5000.\sqrt{2}$.

Figure 4

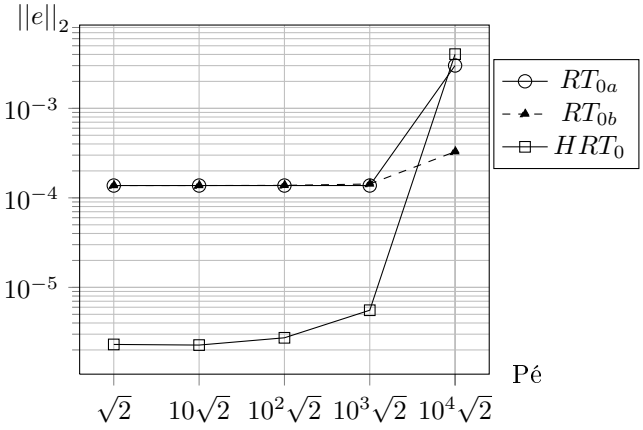

Figure 10: L^2 errors of u in Test 3 for $l = 64$ and increasing Pé

However in contrast one might recall the very bad findings in the case of a curved boundary (cf. Test-problem 1).

CONCLUDING REMARKS

As a conclusion of the tests carried out in the previous section, it can be asserted that the Hermite methods showed an overall behavior better than their mixed analogs. Nevertheless the authors have to make an important remark on the solution of real-life convection-diffusion problems with the methods considered in this study. As they should

Figure 5

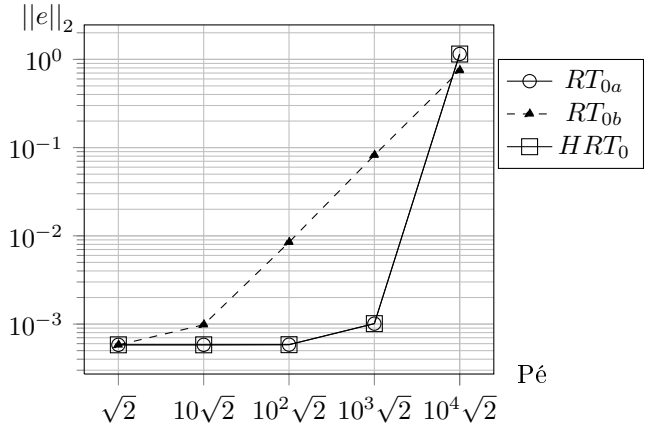

Figure 11: L^2 errors of ∇u in Test 3 for $l = 64$ and increasing Pé

Figure 6

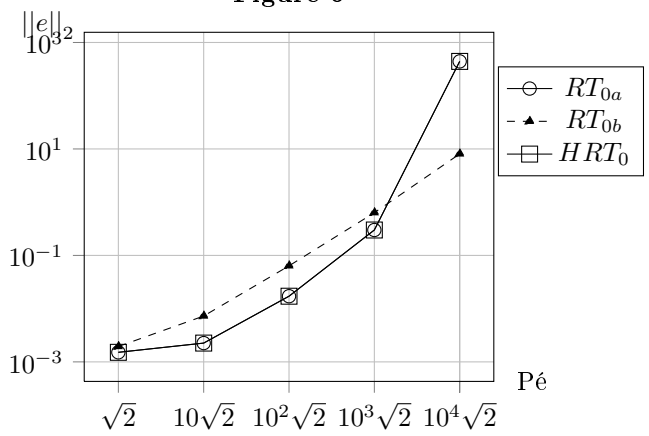

Figure 12: L^2 errors of $DF(u)$ in Test 3 for $l = 64$ and increasing Pé

emphasize, none of them is to be employed as such in the presence of sharp boundary layers, or even simply in finite element simulations of processes at high Péclet numbers. Indeed it is well-known that suitable recipes must be used in order to overcome such a difficulty. One of the most popular is the SUPG formulation first proposed in [2], among many variants or improvements implemented by several authors since then. The proper way to adapt such techniques to the Hermite elements studied in this paper is a subject left for future work.

References

[1] R.A. Adams, Sobolev Spaces, Academic Press, New York, 1975.

[2] A.N. Brooks & T.J.R. Hughes, A streamline upwind/Petrov-Galerkin formulation for convection dominated flows with particular emphasis on the incompressible Navier-Stokes equations, Comp. Meths. Applied Mechanics Engin., **32** (1982), 199-259.

[3] J. Douglas Jr & J.E. Roberts, Comp.& Appl.Maths **1-1** (1982), 91-103.

[4] P.G. Ciarlet, The Finite Element Method for Elliptic Problems, North Holland, Amsterdam, 1978.

[5] P.A. Raviart & J.M. Thomas, Mixed Finite Element Methods for Second Order Elliptic Problems, Lecture Notes in Mathematics, Springer Verlag, **606**, 292-315, 1977.

[6] V. Ruas, Hermite finite elements for second order boundary value problems with sharp gradient discontinuities, Journal of Computational and Applied Mathematics **246** (2013), 234-242.

[7] V. Ruas, D. Brandão & M. Kischinhevsky, Hermite finite elements for diffusion phenomena, J.Comp.Phys.**235** (2013), 542-564.

[8] V. Ruas & P. Trales, A Hermite finite element method for convection-diffusion equations, AIP Proceedings of the 11th Int. Conf. Numerical Analysis and Appl. Maths., T. Simos ed., Rhodes, Greece, 2013.

[9] V. Ruas, Automatic generation of triangular finite element meshes, Computer and Mathematics with Applications, **5-2**, (1979), 125-140.